Chapter in Porous SiC and GaN: Epitaxy, Catalysis, and Biotechnology Applications, ed. R. M. Feenstra and C. E. C. Wood (Wiley, West Sussex, 2008).

Growth of GaN on porous SiC by molecular beam epitaxy

Ashutosh Sagar[a] and R. M. Feenstra
Dept. Physics, Carnegie Mellon University, Pittsburgh, PA, USA
J. A. Freitas, Jr.
Naval Research Laboratory, Electronics Materials Branch, Washington, DC, USA

1. Introduction

One of the major hurdles in the epitaxial growth of high quality GaN thin films is the unavailability suitable substrates. The lack of suitable substrates leads to poor quality epitaxial films with dislocation densities in the range of 10^{10}-10^{12} cm^{-2} for GaN grown on sapphire [1] [2] and SiC [3]. Such high defect densities are detrimental to the device performance; conventional III-V (like GaAs) devices have defect densities about 4 orders of magnitude lower than presently achievable in GaN.

Two important crystal properties that should ideally be closely matched between the GaN and the substrate are the lattice parameter and the coefficient of thermal expansion. Any mismatch between these properties can result in defects in the film (misfit and threading dislocations due to lattice mismatch and cracking or bowing due to the thermal mismatch). An ideal substrate for GaN epitaxy will be a high quality GaN wafer itself, however, this approach is severely limited due to the absence of high quality, large area GaN substrates. Therefore one has to resort to the heteroepitaxial growth of GaN.

Heteroepitaxial growth of GaN is usually performed on sapphire or SiC (13% and 3.4% lattice mismatch, respectively, with GaN). Such a lattice mismatch between GaN and these substrates results in a high dislocation density in the epitaxial films. A variety of techniques have been employed in the past to reduce this high dislocation density and one of the common methods has been to engineer the substrate surface to control, and thus inhibit, the formation of threading dislocations.

An early paper on substrate engineering to control the dislocations in a strained film was published by Luryi and Suhir [4]. Using Si_xGe_{1-x} film growth on Si substrates as a model, they showed that the critical height of the epitaxial film (maximum thickness of the GaN film before dislocations form to relieve strain) can effectively be infinite by using patterned substrates in which epitaxial growth starts only on "seed pads" smaller than a given size. They demonstrated that in

[a] Current address: Intel Corp., Beaverton, OR, USA.

this case, the strain energy per unit area of the film will never exceed the threshold energy needed for creating dislocations, and they showed that such a substrate can be prepared by patterning it prior to the growth so that the epitaxial growth starts on the "seed pads" only. In addition, they suggested that porous Si is a good candidate for this substrate.

These ideas on using patterned substrates lead to several subsequent works exploring the use of nano-sized islands as growth nucleation sites. Such patterned substrates were also shown to be compliant under stress due to lattice mismatch [5]. In this approach, the substrate was patterned (by photolithography for example) into tiny pillars.

Another promising technique recently developed for reducing dislocation density in GaN epitaxial films is lateral epitaxial lateral overgrowth (LEO) [6]. In brief, the LEO technique relies on two specific growth properties: selective area epitaxy and growth anisotropy. Selective area epitaxy corresponds to spatially controlled growth of an epitaxial layer through openings in a masking material which is typically a dielectric film like silicon dioxide or silicon nitride. Growth anisotropy occurs because the diffusing molecular species on the surface are preferentially incorporated at different crystallographic sites so that growth proceeds faster along some crystal directions than others. In the LEO technique, a few microns of GaN is grown on either sapphire or 6H-SiC, followed by deposition of a masking layer, typically SiO_2 or Si_3N_4 deposited using chemical vapor deposition (CVD). Then a set of parallel stripes separated by window areas is opened in the mask by using standard photolithography techniques. Subsequent deposition, under appropriate conditions [7] [8] [9] [10], leads to selective area epitaxy in which the growth is initiated on the GaN layer exposed by the window without any nucleation on the mask layer. Under proper conditions, once the GaN growing film reaches the top of the mask, epitaxial lateral growth *over* the masks starts and finally leads to full coalescence of the film. This technique leads to the filtering of the dislocations by the masks and the lateral overgrown GaN film will be relatively defect free. A schematic of this technique is shown in Fig. 1.

Despite the success of the LEO technique in reducing dislocation density [6], the use of photolithography steps involved in the standard LEO technique makes it a complicated process. A process which can simplify the steps used for preparing a patterned substrate will of great value and the use porous SiC substrates offers such a possibility.

By using porous SiC substrates for GaN epitaxy, selective area epitaxy and lateral overgrowth can potentially be realized on these substrates without the need for any photolithography steps. Figure 2 shows a schematic view of two possible mechanisms by which growth on a porous substrate can lead to defect reduction. For growth by molecular beam epitaxy (MBE), as discussed in this chapter, pores in the substrate often tend to propagate straight up into the film as open tubes, as shown in Fig. 2(a). These open tubes in the GaN film provide

additional free surface where the dislocations can terminate. In addition, if epitaxial growth begins at the areas between the pores, then lateral growth over the pores can result in areas which are dislocation free, as shown in Fig. 2(b).

This chapter is devoted to the discussion of MBE growth of GaN on porous SiC substrates. MBE, compared to CVD, has the advantage of straightforward and well understood nucleation of the GaN on the SiC substrates [3] [11] [12]. On the other hand, the growth temperatures for GaN in MBE, ≈750°C, are significantly less than those in CVD, ≈1020-1050°C, and the resulting lateral growth rates turn out to be much less for MBE (probably because this lateral growth involves significant lateral mass transport over the surface). For this reason, dislocation reduction mechanisms involving lateral overgrowth are expected to be less effective using MBE than CVD. In the present work we do indeed find limited lateral overgrowth in our MBE films; although we observe instances of lateral growth over the pores and concomitant reduced dislocation density in those regions, we do not find any overall dislocation reduction when averaging over the entire area of the films.

In this chapter we first briefly discuss the techniques of porous SiC substrate preparation and some of the relevant properties of the substrates. Following that, we describe the results from our GaN films on the porous SiC substrates, including details of both dislocation mechanisms and strain evolution in the films.

2. Morphology and preparation of porous SiC substrates

2.1 Porous substrates

Porous SiC samples used in this study were purchased from TDI, Inc. They were anodized at a current density of 7mA/cm^2 for 3 min, with a 250 W Hg lamp illuminating 2 in diameter wafers. We used three different types of Si-face (0001) oriented SiC wafers: 6H with no intentional miscut (i.e., on axis), 6H with 3.5° miscut and 4H with 8° miscut. In the latter two cases the miscut was in the $[11\bar{2}0]$ direction.

Figure 3 shows a scanning electron microscopy (SEM) image of a fractured porous 6H-SiC layer, revealing surface pores and the underlying porous network. It is seen in this image that the porosity of the bulk porous network is much less than that of the surface. Transmission electron microscopy (TEM) bright field images of a similar porous layer are shown in the Fig. 4. From these images, we find the pore size (i.e. minimum distance across a pore) of about 20 nm and a bulk porosity of typically 20%-30% for the layers studied here. From Figs. 4(a) and (b), it is also seen that the pores extend downwards in a highly branched structure. In the cross-sectional images, the pores appear like partially open cones. The angle between the upper cone sidewall and a line normal to the (0001) surface is about 75° near the surface, decreasing to 55° at a depth of

about 1.5 μm. Close to the surface the porous layer is not very dense, leading to the existence of a nonporous skin layer. The general morphology of the porous network is quite similar to that described by Zangooie et al. [13].

2.2 Hydrogen etching

As-received porous SiC samples are not ideal as substrates for MBE growth because of polishing damage on the surface. Hydrogen etching is often used to remove such polishing damage [14] [15] [16] [17] [18]. This method involves heating the SiC surface to 1600°-1700°C in hydrogen. In addition, hydrogen etching removes the non-porous skin layer from the top of the porous samples and enlarges the pore sizes. This effect provides us with an effective means of preparing atomically flat samples with controlled surface porosity.

Figure 5 shows a plan view SEM image of 4H SiC sample after hydrogen etching for 60 s at 1680°C. The pores have clearly opened up after the hydrogen etching process; identical results were obtained on 6H SiC samples. The average size of the pores in Fig. 5 is about 100 nm, corresponding to a surface porosity of about 3.5%. Additional hydrogen etching causes the surface porosity to increase further and it also modifies the bulk porous structure. Figure 6(a) is a cross-sectional image of the same sample hydrogen etched for 60 s. It is clear that the bulk pores have opened up after the hydrogen etching process and the network morphology is changed from an unetched sample. The bulk porosity after 60 s of hydrogen etching was about 18% and the average pore size was about 100 nm. The bulk porosity increased to about 24% after 120 s of hydrogen etching and after 300 s of etching the bulk porosity was 31%. The latter case is shown in Fig. 6(b). These observations indicate that the hydrogen etching increasingly opens up the pores with longer etch time. The resulting increase in porosity also has an effect on the hydrogen etch rate; greater porosity providing less surface area for etching in a given horizontal plane and thereby increasing the etch-rate of a porous surface [18].

3. MBE growth of GaN on porous SiC substrates

In this section we will discuss the use of porous SiC substrates for MBE growth of GaN and study its effects on dislocations in the film. We have grown GaN on both porous and nonporous SiC under nominally identical conditions and we provide results on the effect of substrate porosity on the film quality in terms of defect structure and dislocation density. TEM images show that the GaN film grown on porous substrates contains open tubes and a relatively low dislocation density in regions between tubes due to the lateral epitaxial overgrowth. We will discuss various growth mechanisms that can lead to these defect features in the GaN film. We also show the existence of half-loop dislocations at the walls of the open tubes in the GaN films. It is found from the Raman scattering that the GaN

films grown on porous SiC were *not* more strain relaxed compared to those grown on nonporous substrate, despite earlier reports in the literature of the existence of such strain relaxation.

3.1 Experimental details

The porous SiC samples used in this study are the same as described in section 2.1. All our samples used for the GaN growth were 6H polytype with a 3.5° miscut angle. The MBE growth of GaN was performed on the (0001) face of the porous SiC samples under Ga rich conditions [19]. Figure 8(a) shows a plan-view scanning electron microscope (SEM) image of a typical porous SiC surface. The surface pores are 20-50 nm wide. The morphology of the bulk porous layer is as described in section 2.1, where we also discussed the presence of the thin nonporous skin layer, typically ~ 50 nm thick. One means of removing this skin layer is reactive ion etching (RIE) in SF_6 gas, which thus increases the surface porosity without affecting the bulk porous structure [18]. We have used this RIE process to increase the surface porosity of our samples so that, combined with the non-RIE samples, we have a wide range of samples with different surface porosities. Brief (1 min) hydrogen etching was used following the RIE etching to remove surface damage from the wafers although as discussed in section 2.1 the hydrogen etching also affects the pore size (making the pores larger) [18]. For example, Fig. 7(a) shows nano size (20 - 50 nm) pores in a plan-view SEM image of an as-received porous SiC sample. Figure 7(b) is an image of the same sample after it has been hydrogen etched for 1 minute. Figure 7(c) shows another image of a sample from the same wafer, which was reactive ion etched in SF 6 plasma for 6 minutes and then hydrogen etched for 1 minute. Figure 7(d) shows an SEM image of a different sample which was not reactive ion etched but was only hydrogen etched for 1 minute. The surface porosity of our samples was measured simply by counting the number of surface pores after the hydrogen etching. The surface pore density of the samples in Figs. 7(b), (c) and (d) was 3.5, 13 and 11.5 μm^{-2}, respectively. It is important to note that although Fig. 7(b) and (c) show comparable pore density, the porous surface in Fig. 8(c) is much less flat than in Fig. 7(d) because the RIE step exposed the subsurface porous network. Using this combination of RIE and hydrogen etching, we prepared a range of samples with different surface porosities needed for the present study.

After the hydrogen etching, samples were loaded into the MBE chamber. GaN growth was performed in Ga rich condition at the substrate temperature of 750° C. A nitrogen plasma cell was used for nitrogen source and the growth proceeded for 8 hours. After the growth, samples were characterized using x-ray diffraction by measuring the FWHM of the symmetric (0002) and asymmetric $(10\bar{1}2)$ rocking curves to estimate screw and threading dislocation density in the films. TEM images were taken in cross-section to study the dislocations in the GaN films. Also, Raman scattering (RS) data was acquired to verify if any changes in film strain had occurred.

RS is a convenient non-destructive technique to investigate vibrational phenomena in solids. Inelastic light scattering in crystal is susceptible to selection rules resulting from momentum conservation, which limited to the study of optical phonons near the center of the Brillouin Zone. This limitation can be removed by the introduction of impurities, defects, or by fabricating crystals with larger lattice constant along the growth direction than that of the corresponding single crystals, e.g., a superlattice. The use of optical confocal microscope to reduce the laser spot size and increase light collection makes RS spectroscopy (micro-RS) extremely convenient to probe small crystals and thin films.

3.2 Film structure

Figure 8(a) shows a cross-sectional TEM image, viewing along the $[1\bar{1}00]$ direction, of a GaN film grown on nonporous SiC. A high density of threading dislocations was observed to emerge from the GaN/SiC interface and propagate upward during the growth. Figure 8(b) shows the GaN film, viewing along the $[11\bar{2}0]$ direction, grown on a porous SiC surface, whose plan view image is shown in Fig. 4.7(c). As mentioned earlier, the porous SiC substrate shown in Fig. 8(b) was reactive ion etched in SF 6 for 6 minutes, before being hydrogen etched for 1 minute. The surface pore density for the substrate shown in Fig. 4.8(b) is 13 μm^{-2}. The substrate pores in Fig. 8(b) were generally found to be filled with Ga droplets after the GaN growth. GaN nucleates on the pore walls close to the substrate surface and then grows laterally. Such local GaN LEO process caps some of the pore openings. These regions, where the significant lateral growth over the substrate pores has taken place are marked by "D" in Fig. 8, and these regions contain relatively fewer threading dislocations. However, at the openings that are only partially closed by LEO, open tubes can extend vertically all the way to the top surface. These open tubes are marked by "T" in these images. Most of these tubes are partially filled with Ga due to the Ga rich growth conditions. The regions around these tubes have a relatively low density of threading dislocations originating from the film/substrate interface. In the regions around these tubes, dislocation half loops, marked by "a", are seen to punch in horizontally from the tube walls [Fig. 8(c)]. These half loops are also shown in the Figs. 9(a) and (b). This result is in contrast to Fig. 8(a), i.e. for a film grown on a nonporous substrate where the dislocations are mostly created and propagated from the film/substrate interface.

Figure 8(b) is taken under a many-beam condition to reveal all defect features, whereas in Figs. 8(c) and (d) the sample is tilted to reveal strong contrast from the tubes and dislocation loops, respectively, in the same sample area. The GaN film in Figs. 8(c) and (d) was grown on a porous substrate, which was only hydrogen etched for 1 minute, resulting in a surface pore density of 11.5 μm^{-2}, comparable to the substrate in sample shown in Fig. 8(b). Figure 8(c) was imaged with the sample tilted close to a two-beam condition with g=$[\bar{1}103]$, viewing along the $[11\bar{2}0]$ direction. We observed in Fig. 8(c) open tubes originated from essentially all pores at the substrate surface and extended up

through the film, suggesting that lateral overgrowth of GaN has not occurred on such flat porous surface. The dislocation loops are barely visible under the imaging condition in Fig. 8(c). Dislocation half loops are observed, however, in strong contrast in Fig. 8(d) where the same sample is tilted about the c-axis ~30° away from Fig. 8(c) (now viewing along the $[1\bar{1}00]$ direction) and is imaged under a two-beam condition with g=$[\bar{1}\,\bar{1}20]$. This suggests that the half-loop dislocations must have Burgers vector g=1/3<$11\bar{2}0$> as is expected for loops that glide horizontally from the tubes. A loop marked by “a" in Fig. 8(c) is clearly seen to glide out from a tube. We note that the image taken with a horizontal g [Fig. 8(d)] shows no contrast from the tubes. Remarkably, we find maximum contrast from the tubes only when using an inclined g-vector (i.e. not completely horizontal or vertical). Strain variations around the open tubes should play some role in determining the contrast.

Figure 10 shows a plot of symmetric and asymmetric rocking curve FWHM of GaN film as a function of substrate pore density. On average, there does not seem to be any significant improvement in the x-ray FWHM for the films grown on the various porous substrates. In particular, for the symmetric rocking curves, the values for films on porous substrates are significantly greater than for growth on nonporous substrates (i.e. at zero pore density); the latter are exceptionally low since our GaN films on SiC have a very low density of dislocations with [0002] component in their Burgers vector [3]. Aside from this difference, the x-ray rocking curve results do not show a significant variation with surface pore density of the substrate. Since the x-ray FWHM is a measure of the mosaic structure and strain variation in a large area of the film (due to the beam size ~1 mm^2) and also through the entire thickness of the GaN film, this value is not a true indication of the defect structure and growth mechanisms working at the nano-scale. Even though x-ray results are not significantly improved for growth on the porous substrates, TEM images discussed earlier show that the porous substrate is able to produce local areas in the GaN film having relatively low defect density.

3.3 Film strain

In addition to defect density, another important characteristic of heteroepitaxial growth of the mismatched materials is the degree of strain relaxation in the film compared to the substrate. It was found in previous work that use of porous substrates can lead to significant strain relaxation in the film, at least in certain cases [20] [21].

The hexagonal crystalline phase of GaN, or wurtzite structure, belongs to the space group C^4_{6v}, and has two molecules per Brillouin unit cell. Group theory predicts eight zone center optical phonon modes, represented by $1A_1$(TO), $1A_1$(LO), $2B_i$, $1E_1$(TO), $1E_1$(LO), and $2E_2$. The two B_1 are silent modes, or Raman inactive, but all the six allowed first order phonons have been observed in thin films [22]. These phonons have also been observed in thick and high quality

freestanding HVPE GaN substrates and their energy have been used for estimate the biaxial stress in our samples [23].

To verify the strain relaxation of our GaN films we have carried out micro Raman spectroscopy, which is performed in a backscattering geometry, with the results shown in Fig. 11. Spectrum (a) shows the result for a GaN film grown on nonporous SiC, and spectra (b) – (d) show results for films on porous SiC. The observed location of the GaN E_2 line near 567 cm^{-1} is nearly the same in all cases; from Gaussian fitting we find locations of 566.7, 566.7, 566.5, and 566.8 cm^{-1} for spectra (a) – (d), respectively, with an error of ± 0.1 cm^{-1} for each measurement. The Raman line positions are thus essentially the same for all samples, demonstrating no additional strain relaxation for the films grown on the porous substrates. Generally, MBE-grown GaN films on SiC tend to have a small amount of compressive strain arising from the lattice mismatch between GaN and SiC (the thermal mismatch leads to tensile strain, but this effect is smaller) [24]. Indeed, from wafer curvature measurements we observe some residual compressive strain for our films grown on the porous substrates (for the films grown on nonporous substrates the curvature measurements were hindered by the presence of a molybdenum film on the backside of the wafers, leading to artifacts in the results) [25]. Strain measurements by electron diffraction during TEM have also been done on such films [19]; some difference in strain were observed in that case between films grown on nonporous and porous substrates, although differences in growth temperature for those samples could affect those results [24].

We conclude that the porosity of the SiC substrate has only a small, or zero, effect on the strain in the GaN films. This conclusion is, perhaps, not surprising when we carefully consider the geometry of the situation. The prior work which *did* observe a strain reduction was for GaN growth on porous GaN, employing a GaN buffer layer that was then etched to make it porous [20] [21]. It was found that the pores extended vertically down into the layer, i.e. following the columnar nature of the film [20]. By removing material from around the columns, the material inside the columns can elastically relax (so long as the depth of the etched material is comparable to the width of the column). Subsequent overgrowth then led to a reduced strain level in the film. In contrast, for the present experiments it is the SiC substrate that is porous, with the GaN grown epitaxially on that. The GaN will be strained by its mismatch to SiC, and there is no real mechanism associated with the porosity for this strain to be relaxed. It is important to realize in this regard that the porous SiC itself is very rigid (removing some material to make it porous will lead to only a small decrease in its elastic constants), and hence in no way can it act as a type of “compliant” substrate. Hence, no significant strain relaxation in the GaN film is found.

Another manifestation of the strain in the films is the presence of the half-loop dislocations extending out from the open tubes in the GaN films grown on the porous substrates, as discussed in the previous section. Regarding the origin of

these half-loops, it is easy to see that open tubes (or voids) in a strained film will act as stress concentrators: Since the normal component of the stress is necessarily zero at the tube wall, the material near the wall will be displaced relative to its position in the absence of the void, and the tangential in-plane component of the stress is thereby increased. In other words, during growth, the shear stress field of the GaN film will be locally concentrated around these open tubes in the film. The open tubes provide a free surface where these half-loops can nucleate due to the increased stress.

We have performed finite element analysis on a simple model to demonstrate the concentration of shear stress around the pore wall. Figure 12(a) shows the model used and Fig. 12(b) is a plot of shear stress as a function of distance from the pore wall. It is evident that there is considerable stress concentration in the film around the substrate pores, which can lead to the formation of the half loop dislocations.

4. Summary

In this chapter, we have discussed the MBE growth of GaN on porous SiC. We discussed the morphology of porous SiC and the effect of hydrogen etching on substrate porosity. It was seen that the MBE grown GaN film on porous SiC has open tubes extending over the substrate pores, and we observed the instances of lateral epitaxial overgrowth GaN films over the porous substrates. We have shown, with cross-sectional TEM images that in the regions of lateral epitaxial overgrowth, the GaN films on porous SiC substrates have low dislocation density. However, we did not find any overall improvement in the FWHM of the symmetric and asymmetric x- ray rocking curves on these GaN films grown on substrates with different porosities. In addition, it was found from Raman spectra that the films on porous SiC were not significantly strain relaxed compared to the films on nonporous substrates.

5. Acknowledgements:

This work was supported by the DURINT program administered by the Office of Naval Research (Dr. C. Wood) under Grant N00014-0110715. We are grateful to Dr. T. S. Kuan for collaboration and numerous stimulating discussions.

6. References:

[1] D. Kapolnek, X. H. Wu, B. Heying, S. Keller, B. P. Keller, U. K. Mishra, S. P. Denbaars, "Structural evolution in epitaxial metalorganic chemical vapor deposition grown GaN films on sapphire", Appl. Phys. Lett. **67**, 1541 (1995).

[2] S. Keller, B. P. Keller, Y. -F. Wu, B. Heying, D. Kapolnek, X. H. Wu, J. S. Speck, U. K. Mishra and S. P. Denbaars, "Influence of sapphire nitridation on properties of gallium nitride grown by metalorganic chemical vapor deposition", Appl. Phys. Lett. **68**, 1525 (1996).

[3] C. D. Lee, V. Ramachandran, 6, A. Sagar, R. M. Feenstra, D. W. Greve, W. L. Sarney, L. Salamanca-Riba, D. C. Look, Song Bai, W. J. Choyke and R. P. Devaty, "Properties of GaN epitaxial layers grown on 6H-SiC(0001) by plasma-assisted molecular beam epitaxy ", J. Electron. Mater. **30**, 162 (2001).

[4] Serge Luryi and Ephrahim Suhir, "New approach to the high quality epitaxial growth of lattice-mismatched materials", Appl. Phys. Lett. **49**, 140 (1986).

[5] D. Zubia and S. D. Hersee, "Nanoheteroepitaxy: The Application of nanostructuring and substrate compliance to the heteroepitaxy of mismatched semiconductor materials", J. Appl Phys. **85**, 6492 (1999).

[6] E. Frayssinet, B. Beaumont, J. P. Faurie, Pierre GIBART, Zs. Makkai, B. Pecz, P. Lefebvre, P. Valvin, "Micro Epitaxial lateral overgrowth of GaN/sapphire by Metal Organic Vapour Phase Epitaxy ", MRS Internet J. Nitride Semicon. Res. **7**, 8 (2002).

[7] T. S. Zheleva, O. -H, Nam, M. D. Bremser and R. F. Davis, "Dislocation density reduction via lateral epitaxy in selectively grown GaN structures", Appl. Phys. Lett. **71**, 2472 (1997).

[8] A. Sakai, H. Sunakawa and A. Usui, "Defect structure in selectively grown GaN films with low threading dislocation density", Appl. Phys. Lett. **71**, 2259 (1997).

[9] S. Kuarai, K. Nishino and S. Sakai, "Nucleation Control in the Growth of Bulk GaN by Sublimation Method", Jpn. J. Appl. Phys., **36**, L184 (1997).

[10] J. Wang, S. Tottori, H. Sato, M. -S. Hao, Y. Ishikawa, T. Sugahara, K. Ya-mashita and S. Sakai, "Lateral Overgrowth of Thick GaN on Patterned GaN Substrate by Sublimation Technique", Jpn. J. Appl. Phys. **37**, 4475 (1998).

[11] Masato Ebihara, Satoru Tanaka and Ikuo Suemune, "Nucleation and Growth Mode of GaN on Vicinal SiC Surfaces", Jpn. J. Appl. Phys., **46**, L348 (2007).

[12] P. Waltereit, S.-H. Lim, M. McLaurin, J.S. Speck, "Heteroepitaxial Growth of GaN on 6H-SiC(0001) by Plasma-Assisted Molecular Beam Epitaxy", phys. stat. solidi (a) **194**, 524 (2002).

[13] S. Zangooie, J. A. Woolam, and H. Arwin, "Self-organization in porous 6H-SiC", J. Mater. Res. **15**, 1860 (2000).

[14] C. Hallin, A. S. Baskin, F. Owman, P. Martensson, O. Kordina and E. Jangen, "Study of the hydrogen etching of silicon carbide substrates", Silicon Carbide and related materials 1995, Kyoto, Japan, Inst. Phys. Conf. Ser. No. **142,** (IOP, Bristol, 1996), Chap. 3.

[15] T. L. Chu and R. B. Campbell, "Chemical Etching of Silicon Carbide with Hydrogen", J. Electrochem. Soc. **112**, 955 (1965).

[16] V. Ramachandran, M. F. Brady, A. R. Smith and R. M. Feenstra, "Preparation of atomically flat surfaces on silicon carbide using hydrogen etching", J. Electron. Mater. **27**, 308 (1998).

[17] C. D. Lee, R. M. Feenstra, O. Shigiltchoff, R. P. Devaty and W. J. Choyke, "Structural Properties of GaN Films Grown by Molecular Beam Epitaxy on Singular and Vicinal 6H-SiC(0001)", MRS Internet J. Nitride. Semicond. Res. **7**, 2 (2002).

[18] A. Sagar, C. D. Lee, R. M. Feenstra, C. K. Inoki and T. S. Kuan, "Morphology and effects of hydrogen etching of porous SiC", J. Appl. Phys. **92**, 4070 (2002).

[19] C. K. Inoki, T. S. Kuan, C. D. Lee, A. Sagar and R. M. Feenstra, D. D. Koleske, D. J. Diaz, P. W. Bohn, and I. Adesida", Growth of GaN on porous SiC and GaN substrates", J. Electron. Mater., **32**, 855 (2003).

[20] M. Mynbaeva, A. Titkov, A. Kryganovskii, V. Ratnikov, K. Mynbaev, H. Huhtinen, R. Laiho, and V. Dmitriev", Structural characterization and strain relaxation in porous GaN layers", Appl. Phys. Lett. **76**, 1113 (2000).

[21] B. K. Ghosh, T. Tanikawa, A. Hashimoto, A. Yamamoto, and Y. Ito, "Reduced-stress GaN epitaxial layers grown on Si(111) by using a porous GaN interlayer converted from GaAs", J. Cryst. Growth **249**, 422 (2003).

[22] J.A. Freitas, Jr. and M.A. Khan, “Raman and photoluminescence studies of undoped and magnesium-doped GaN films on sapphire”, Mat. Res. Soc. Symp. Proc. **339**, 547 (1994).

[23] J.A. Freitas, Jr., "Optical studies of bulk and homoepitaxial films of III–V nitride semiconductors", J. Cryst. Growth **281**, 168 (2005).

[24] B. J. Skromme, H. Zao, D. Wang, H. S. Kong, M. T. Leonard, G. E. Bulman, and R. J. Molnar, "Strain determination in heteroepitaxial GaN", Appl. Phys. Lett. **71**, 829 (1997).

[25] A. Sagar, C. D. Lee, R. M. Feenstra, C. K. Inoki, and T. S. Kuan, "Plasma-assisted molecular beam epitaxy of GaN on porous SiC substrates with varying porosity", J. Vac. Sci Technol. B **21**, 1812 (2003). Regarding the wafer curvature results reported in this work, the results for nonporous substrates are in error since those substrates had a coating of molybdenum on their backside that itself induced significant curvature in the substrate. This coating was absent for the films grown on the porous substrates.

Figures:

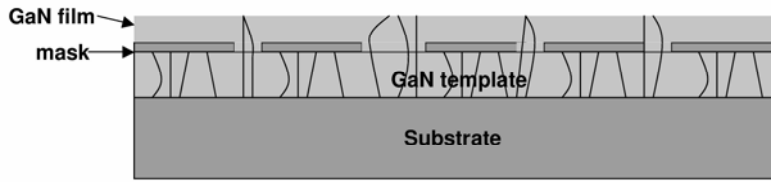

Figure 1. A schematic of the lateral epitaxial overgrowth technique for growing defect free GaN. The black lines extending from the substrate to the top of the film represent dislocations.

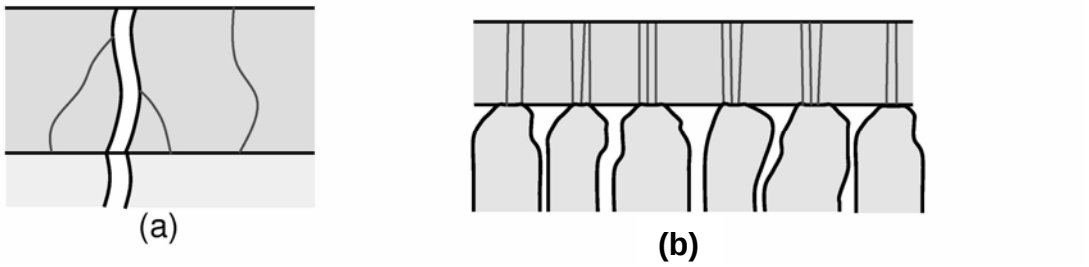

Figure 2. Schematic illustration of two defect reduction mechanisms for a strained film (dark gray) grown on a porous substrate (light gray). (a) Dislocations bending toward the open surface at the tube walls. (b) Formation of relatively dislocation free regions in the GaN film where the film has laterally grown over the pores.

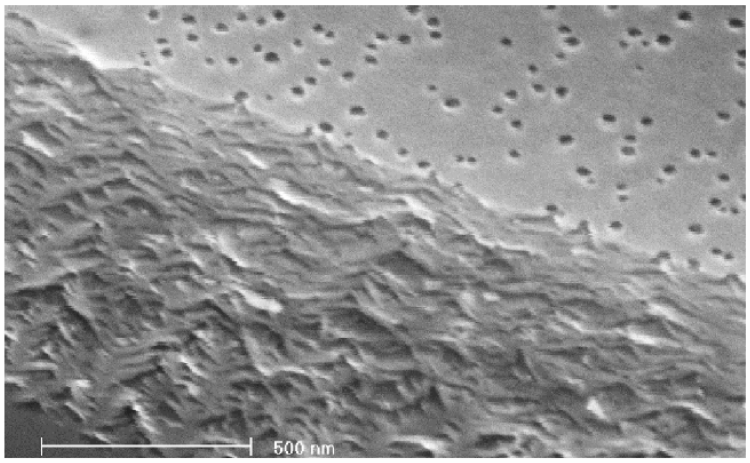

Figure 3: Cross-sectional SEM image of the porous 6H-SiC. The sample was tilted to allow simultaneous viewing of the porous network in cross-section along with the pores on the top surface. Pore formation starts at the surface and then it develops into an inverted V-shaped branched structure in the bulk.

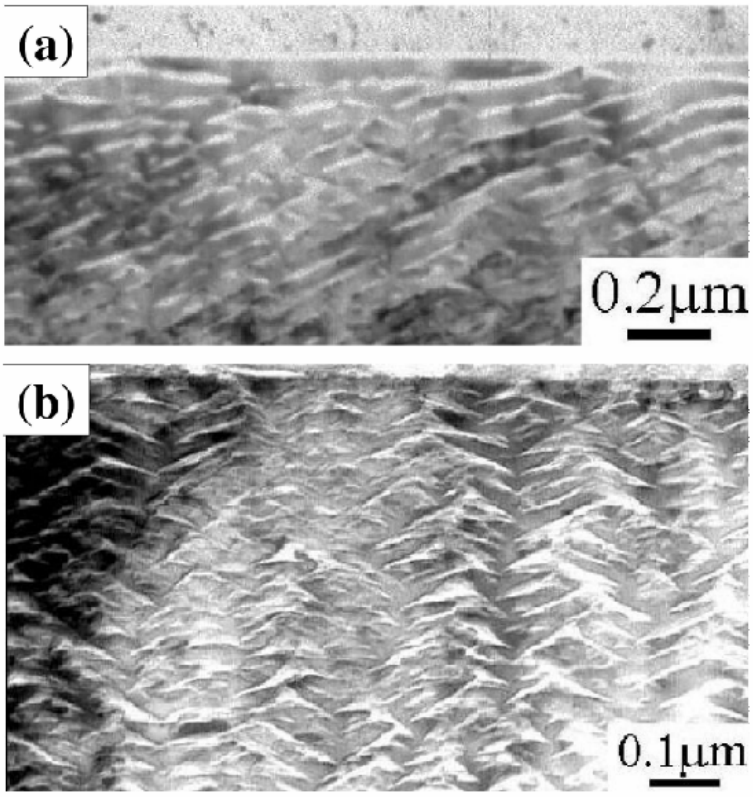

Figure 4: Cross sectional TEM images of two porous layers. There are relatively few pores on the surface compared to the bulk, with the top skin layer being most clearly visible in (a). The V-shaped branched structure of the porous network is clearly seen in (b).

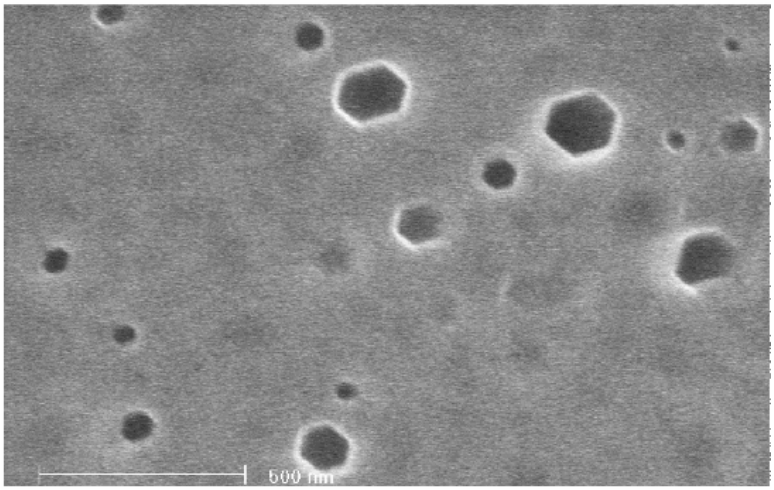

Figure 5: Plan - view SEM image of the hydrogen etched surface of porous 4H-SiC. Pores have opened up after 60 s of hydrogen etching at 1680°C. The average pore size is about 100 nm and the surface porosity is about 3.5%.

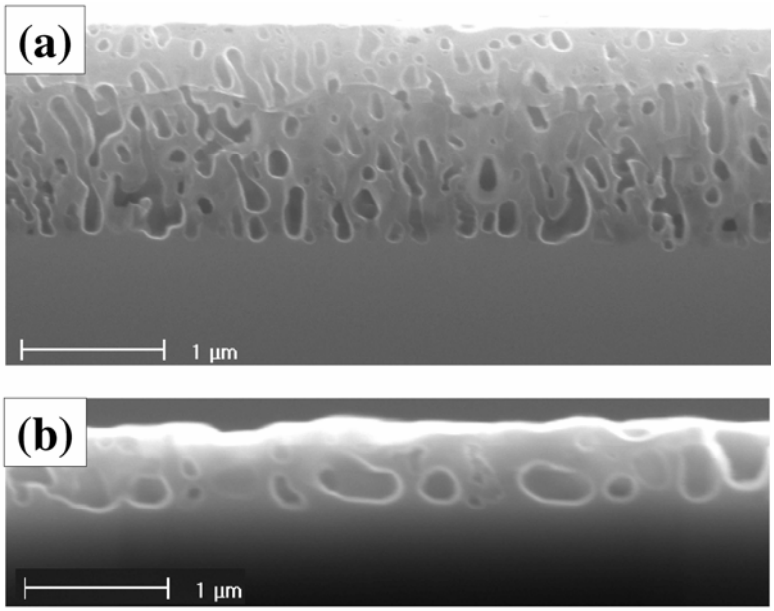

Figure 6: Cross-sectional SEM images of porous 4H-SiC, hydrogen etched at 1680°C for (a) 60 s and (b) 300 s. The bulk porosity is about (a) 18% and (b) 31%. The pores have enlarged due to the hydrogen etching.

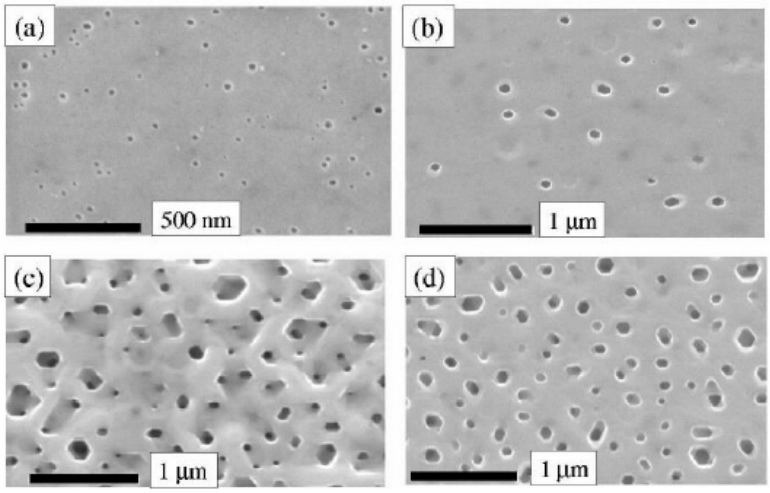

Figure 7: Plan view SEM images of porous SiC surfaces: (a) as-received porous surface without any surface etching treatment, (b) the surface after hydrogen etching for 1 min at 1700°C, (c) the surface after reactive ion etching in SF_6 for 6 minutes followed by hydrogen etching for 1 minute at 1700°C. Images (a) – (c) refer to the same wafer, after various processing steps. Image (d) is from a different wafer, prepared by hydrogen etching at 1700°C for 1 minute.

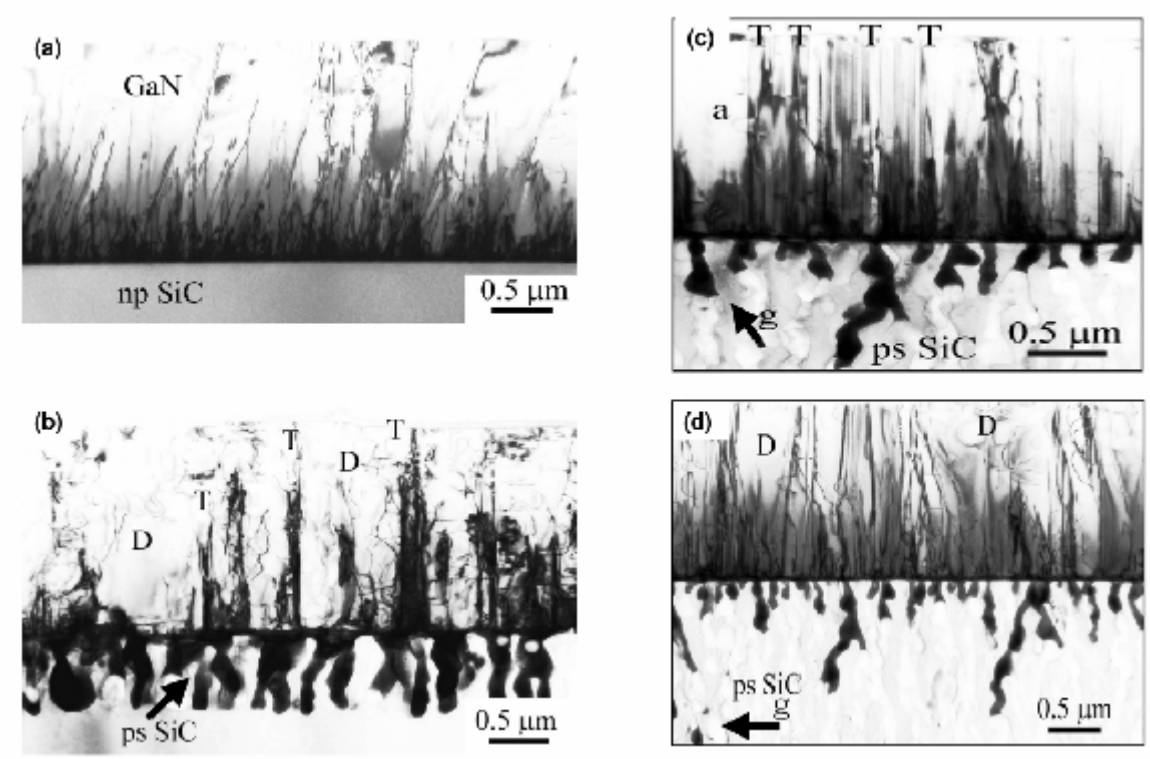

Figure 8: Cross-sectional TEM images of GaN films on (a) nonporous SiC substrate, and (b) – (d) on porous SiC substrates. The label "ps" denotes a porous substrate and "np" denotes a nonporous substrate. The surface pore density of the substrate in (b) is 13 μm^{-2}, and in (c) and (d) is 11.5 μm^{-2}. The open tubes in the GaN films on porous substrates are marked by "T" (the tubes appear white in contrast near the top of the film where they are empty, and black near the interface where they are filled by Ga). The regions labeled by "D" contain a relatively low number of threading dislocations originating at the interface (due to the lateral epitaxial growth over the substrate pores), and they contain dislocation half-loops gliding in from tubes. One half-loop is faintly seen to the right of "a" in (c).

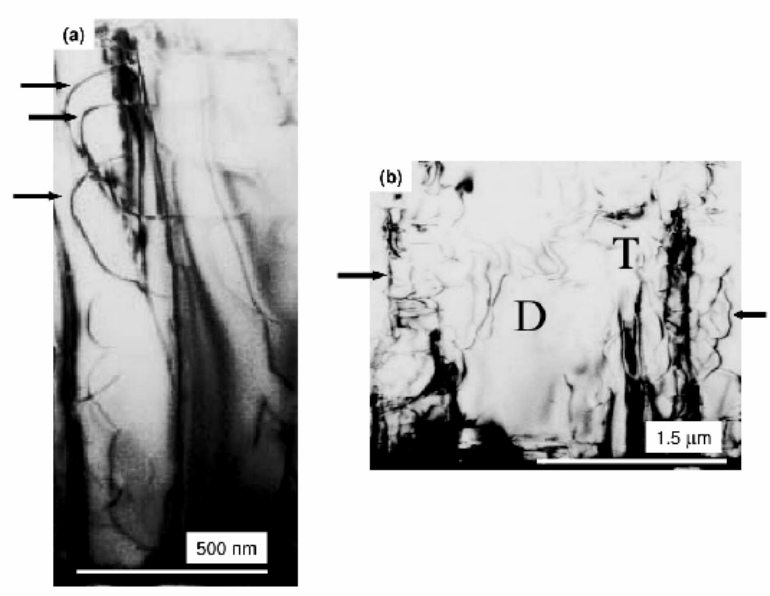

Figure 9: Magnified images of GaN on porous 6H SiC. The half loops are clearly seen in (a), with some of them indicated by arrows. The region marked by "D" in (b) shows nearly defect free GaN due to the lateral epitaxial growth over the pores. The open tubes are marked by "T".

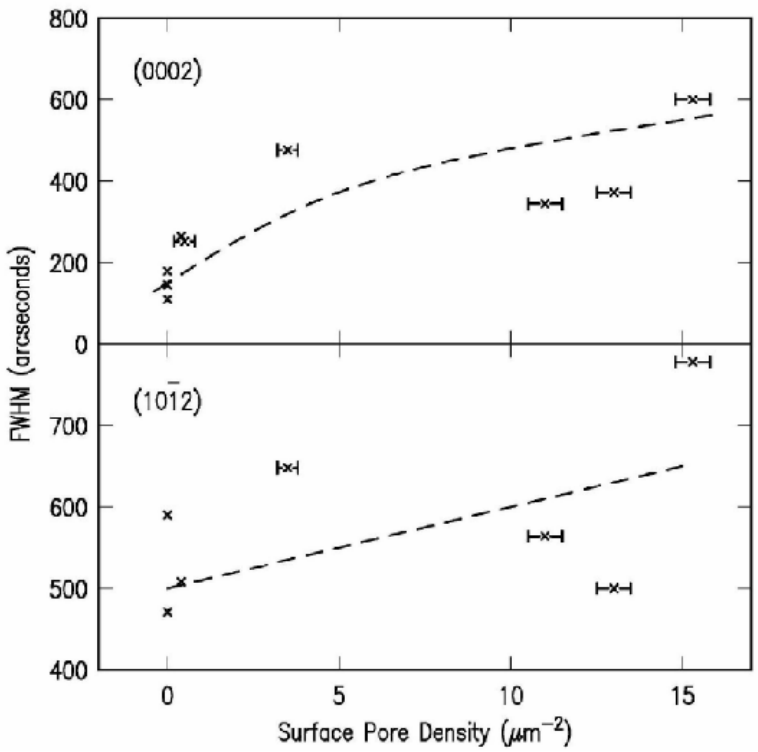

Figure 10: Triple axis symmetric (0002) and asymmetric $(10\bar{1}2)$ x-ray rocking curve FWHM of the GaN films grown on porous SiC. The horizontal axis shows the density of surface pores on various substrates. The dashed lines are drawn as guides to the eye.

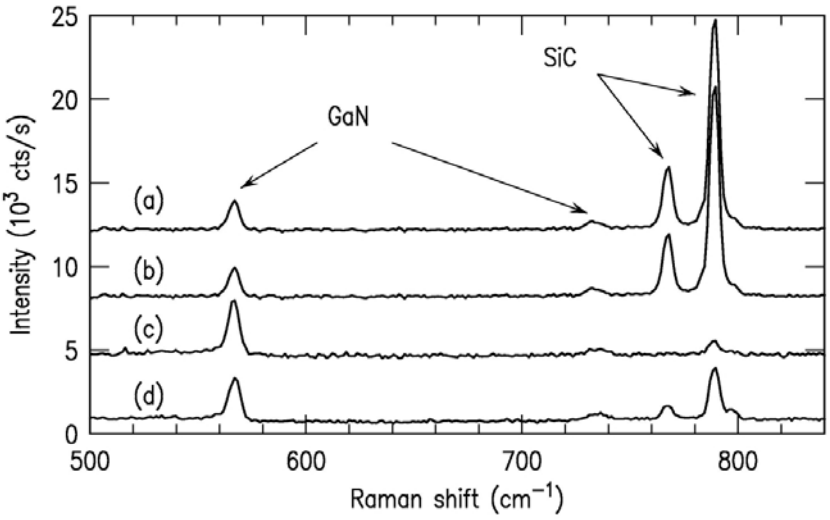

Figure 11. Raman spectroscopy of GaN films grown on (a) nonporous and (b) – (d) porous SiC substrates. Raman shifted lines due to the SiC substrate and due to the GaN film are resolved. The zero intensity level in consecutive spectra are shifted for ease of viewing.

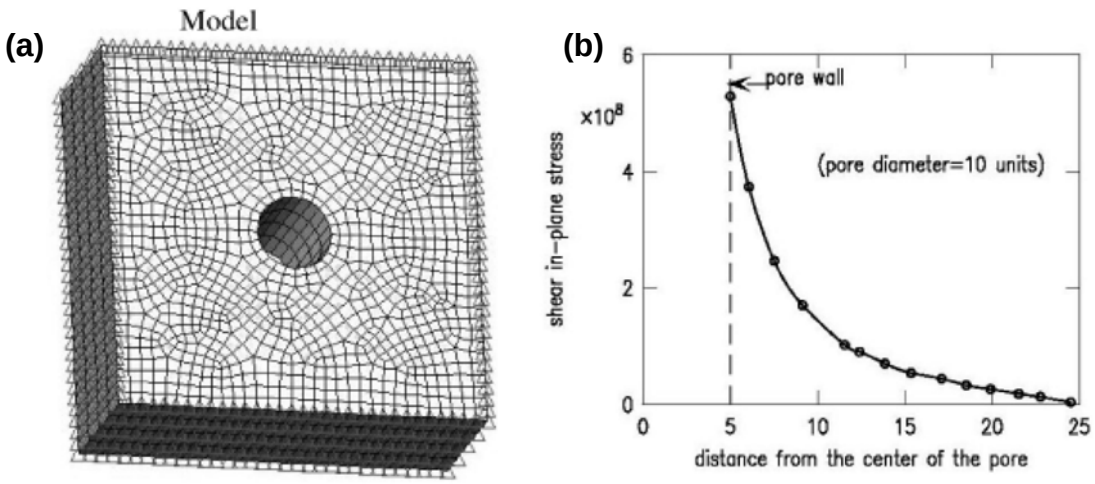

Figure 12: Finite element analysis of shear stress distribution around a circular pore under biaxial stress. (a) The finite element analysis model, showing a single circular pore in a solid brick. (b) Plot of shear stress along a diagonal line in model as a function of distance from pore wall. The units are arbitrary and the length scale of the stress field is determined by the pore diameter in the model (10 distance units).